PCCP

Non-equilibrium steady state conductivity in cyclo[18]carbon and its boron nitride analogue

Journal:	*Physical Chemistry Chemical Physics*
Manuscript ID	CP-ART-08-2020-004172.R1
Article Type:	Paper
Date Submitted by the Author:	21-Sep-2020
Complete List of Authors:	Raeber, Alexandra; University of Chicago, Deparment of Chemistry Mazziotti, David; University of Chicago, Chemistry

SCHOLARONE™
Manuscripts

Non-equilibrium steady state conductivity in cyclo[18]carbon and its boron nitride analogue

Alexandra E Raeber and David A Mazziotti[*]

Department of Chemistry and The James Franck Institute,
The University of Chicago, Chicago, IL 60637 USA

(Dated: Submitted August 6, 2020)

A ring-shaped carbon allotrope was recently synthesized for the first time, reinvigorating theoretical interest in this class of molecules. The dual π structure of these molecules allows for the possibility of novel electronic properties. In this work we use reduced density matrix theory to study the electronic structure and conductivity of cyclo[18]carbon and its boron nitride analogue, B_9N_9. The variational 2RDM method replicates the experimental polyynic geometry of cyclo[18]carbon. We use a current-constrained 1-electron reduced density matrix (1-RDM) theory with Hartree-Fock molecular orbitals and energies to compute the molecular conductance in two cases: (1) conductance in the plane of the molecule and (2) conductance around the molecular ring as potentially driven by a magnetic field through the molecule's center. In-plane conductance is greater than conductance around the ring, but cyclo[18]carbon is slightly more conductive than B_9N_9 for both in-the-plane and in-the-ring conduction. The computed conductance per molecular orbital provides insight into how the orbitals—their energies and densities—drive the conduction.

I. INTRODUCTION

The structure and properties of ring-shaped carbon allotropes, known as cyclo[n]carbons, have been of theoretical interest for many years, first appearing in the literature more than fifty years ago [1]. As a result of their sp hybridization, cyclo[n]carbons have two orthogonal π systems, allowing for the possibility of double aromatic stabilization [2, 3]. Their high reactivity, however, means that their synthesis was not possible until very recently. Last year, the first of these carbon allotropes, cyclo[18]carbon, was synthesized and characterized using high-resolution atomic force microscopy [4].

Prior to its synthesis, two possible structures had been hypothesized for cyclo[18]carbon, a cumulenic form, without bond length alternation, and a polyynic form, with alternating single and triple bonds. The cumulenic structure, which is predicted by Hückel theory, is generally found to be the lowest in energy by density functional theory (DFT) [5–7] and Møller-Plesset second-order perturbation theory [8] calculations. The polyynic structure, on the other hand is supported by Hartree-Fock [9, 10], Monte-Carlo [11], and coupled cluster calculations [12]. Recent experimental work confirmed the polyynic geometry to be correct [4, 13, 14].

Boron nitride (BN) forms hexagonal lattices which are isoelectric to those formed by carbon. Its two-dimensional hexagonal lattice is analogous to graphene and has high thermal and chemical stability [15]. Theoretical work on boron nitride analogues to cyclo[n]carbons has shown that they may have similar novel properties with higher stability [16–18].

Here we study the electronic structure and molecular conductivity of the cyclo[18]carbon and B_9N_9 molecules

using reduced density matrix (RDM) theory [19–25]. Computations with the variational two-electron reduced density matrix (2-RDM) method [19–23], which can treat fractionally filled orbitals and strong electron correlation if present [26–28], reveal that neither molecule is strongly correlated and support the experimental polyynic structure of cyclo[18]carbon. Using a current-constrained 1-electron reduced density matrix (1-RDM) theory with the Hartree-Fock molecular orbitals and energies [24, 25], we compute the intrinsic molecular conductance of both molecules in two cases: (1) conductance in the plane of the molecule and (2) conductance around the molecular ring as potentially driven by a magnetic field through the molecule's center.

We find for both cyclo[18]carbon and B_9N_9 that conductance in the plane of the molecule is greater than conductance around the ring. Furthermore, cyclo[18]carbon is slightly more conductive than B_9N_9 for both (1) and (2). The intrinsic conductance provides information about the intrinsic ability of a molecule to support conductance that does not consider the resistance from the junction or lead. Intrinsic conductance is useful for assessing whether a molecule is a potentially good molecular conductor or insulator prior to optimization of the lead and/or junction. The conductance per molecular orbital is also obtained, providing insight into how the orbitals—their energies and densities—drive the conduction.

II. THEORY

The idea of creating single molecule circuit elements has been of scientific interest for nearly fifty years [29], with a great deal of progress being made in the past twenty years [30–32]. Traditional theories of molecular conductivity add a voltage to the molecule to compute the current [33–42]. In the current-constrained RDM the-
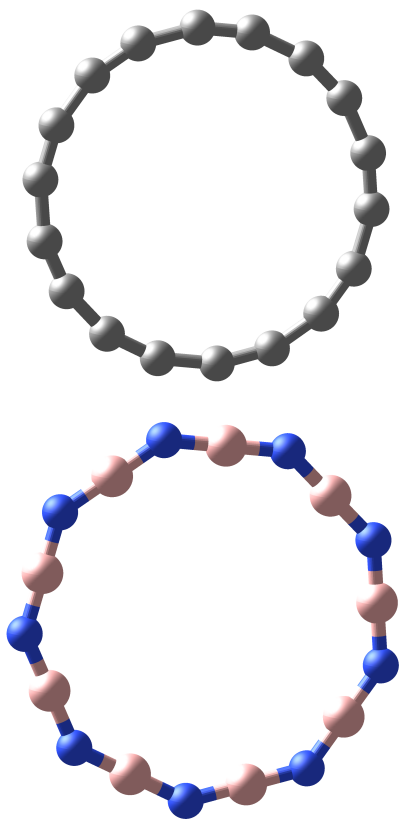
FIG. 1. Ball and stick representations of C_{18} (top) and B_9N_9 (bottom)

ories the current is added as a constraint to compute the reorganization energy and the voltage [24, 25]. This change in paradigm allows us to compute an intrinsic conductance (or resistance) for each molecule that depends only upon a molecule's energetic response to the imposed current constraint, as well as its intrinsic properties such as length and polarization. The intrinsic resistance reflects key qualitative features of molecular conductivity, features that are determined mainly by the electronic properties of the molecule.

To define a 1-RDM theory of molecular conductivity, we begin with the variational principle in the absence of electron transport. The energy of the system, given by

$$E = \mathrm{Tr}(^1K\,^1D), \qquad (1)$$

where ^1K is the matrix form of the one-electron reduced Hamiltonian, which we approximate as the Fock matrix and ^1D is the 1-RDM. This energy is minimized subject to ensemble N-representability conditions on the 1-RDM known as the 1-positivity constraints, which ensure that the 1-RDM generated in the minimization arises from the integration of at least one N-electron ensemble density matrix [23, 43–47]. These conditions have the form,

$$^1D \succeq 0 \qquad (2)$$

$$^1Q \succeq 0 \qquad (3)$$

where ^1D and ^1Q are the one-particle and one-hole reduced density matrices and the symbol $\succeq$ indicates that they must remain positive semidefinite, that is, they must have non-negative eigenvalues. These conditions are equivalent to the Pauli exclusion principle, which restricts the occupation of each spin orbital to lie between 0 and 1. This method of energy minimization is a special type of convex optimization known as semidefinite programming (SDP) [20, 22, 23, 48].

To set the current for the system, we define the one-electron current matrix as the matrix representation of the one-electron gradient in a specified direction $\hat{\kappa}$, given by

$$^1J_q^p = \frac{1}{L}\int_{dr}\phi_p(r)(\nabla\cdot\hat{\kappa})\phi_q(r)dr, \qquad (4)$$

where L is the length of the molecule, r represents the electronic coordinates, $\hat{\kappa}$ is the vector direction of the current, and ϕ_p are the molecular orbitals [24]. We add this to the energy minimization by requiring that

$$\mathrm{Tr}(^1J\,\mathrm{Im}(^1D)) = I, \qquad (5)$$

where I is the current.

In order to investigate the conductivity in the ring rather than across it, changes are made to the form of the one-electron current matrix. For the ring current calculations,

$$^1\tilde{J}_q^p = \left(\sum_i^M L^{-1}\int_{dr}\phi_p(r)(\nabla\cdot\hat{\kappa}_i)\phi_q(r)dr\right)M^{-1}, \qquad (6)$$

where M is the number of atoms in the ring and κ_i is the unit vector tangent to the center of each atom.

III. RESULTS AND DISCUSSION

A. Electronic Structure

Molecular geometries of C_{18} and B_9N_9 as shown in Fig. 1 are obtained by optimization at the v2RDM-CASSCF/cc-pVDZ level of theory [19–23, 49] with an active space of 18 electrons in 18 orbitals, using the SNOPT sequential quadratic programming algorithm [50] with analytical gradients [51] implemented in the Quantum Chemistry Package [52] in Maple [53]. The v2RDM method predicts the experimental polyynic structure, with alternating carbon-carbon bond lengths of 1.50 Å and 1.22 Å. The calculated structure of B_9N_9 agrees well with the DFT structure from recent previous work [18], with a boron-nitrogen bond length of 1.32 Å. The Cartesian coordinates of the optimized geometries are provided in the Supporting Information.

One of the key features of C_{18} is its dual π system, which is well represented in the v2RDM results, with π-type active molecular orbitals which lie either in the plane of the molecule or perpendicular to it. A representative
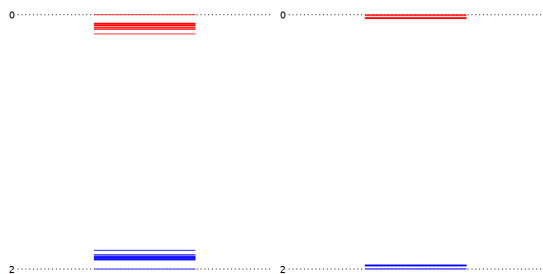
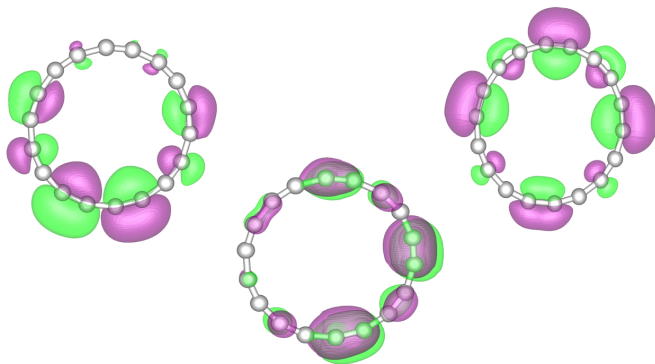FIG. 2. NO occupations of C_{18} (left) and B_9N_9 (right)

FIG. 4. A sample of the active space molecular orbitals for B_9N_9

FIG. 3. A sample of the active space molecular orbitals for C_{18}

FIG. 5. Voltage plotted as a function of current for C_{18} ring (red circle), C_{18} in-plane (red plus), B_9N_9 ring (blue circle), B_9N_9 in-plane (blue plus).

subset of the active orbitals is shown in Fig. 3. Our calculations indicated that this dual π system is shared by B_9N_9, with a representative subset shown in Fig. 4.

We also find that these molecules do not have a high level of static correlation. The natural orbital occupations in the active space, as shown in Fig. 2, do not diverge much from a completely filled (2) or empty (0) state. The occupation of the highest occupied natural orbital (HONO) is 1.85 and the occupation of the lowest unoccupied natural orbital (LUNO) is 0.15. B_9N_9 displays even less static correlation than C_{18}, with a occupation of 1.97 in the HONO and occupation of 0.03 in the LUNO. The minimal static correlation in these molecules supports the computation of their molecular conductivity within a 1-RDM theory.

B. Molecular Conductivity

We investigate the intrinsic conductance both around the molecular ring and in the plane of the molecule for cyclo[18]carbon and B_9N_9. All molecules are centered at the origin and the vector direction $\hat{\kappa}$ of the current is set as the x-axis for the calculation of the in-plane current and as described in the theory section for the ring current. We generate the Hamiltonian using the Fock matrix from a minimization of the Hartree-Fock energy of each molecule in the cc-pVDZ basis set. The energy of the
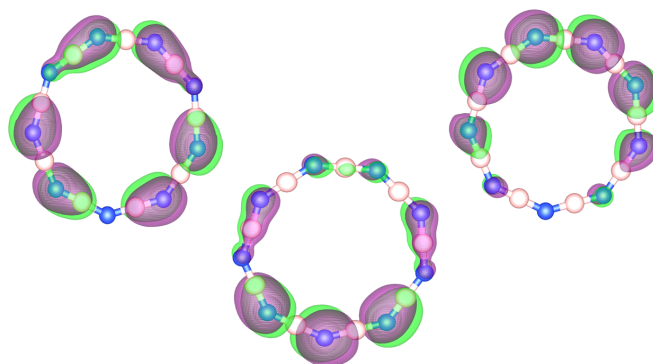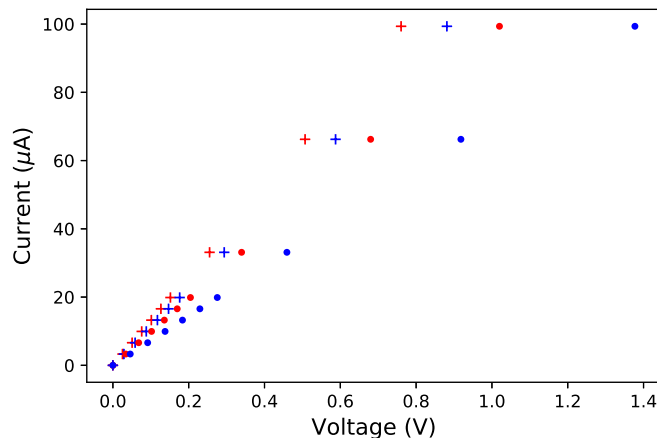
current-constrained steady state is minimized subject to the conditions given in Eqs. (2-4) using semidefinite programming. The current constraint generates a complex-valued SDP that can be mapped to a real-valued SDP by representing the complex matrix by a larger real-valued matrix. Solving this semidefinite program generates the reorganization energy due to the current constraint. The voltage is calculated from this energy by analogy with the molecule's energetic response to an electric field, as described in previous work by the authors [25]. All calculations are performed at 0 K. Since we are interested in a qualitative description of the conductivity which arises only from the molecule itself, we compute the intrinsic conductance of the molecule, omitting the thiol linkers and metal leads present in an experimental molecular junction.

As shown in Fig. 5 we find that cyclo[18]carbon is the more conductive of the two molecules, with a ring conductance of 97.42 μS and a in-plane conductance of 130.64 μS compared to a ring conductance of 72.14 μS and a in-plane conductance of 112.73 μS for B_9N_9.

The lower conductance of B_9N_9 is expected based on the larger energy gap between its highest occupied molecular orbital (HOMO) and lowest unoccupied molecular orbital (LUMO), with a gap of 13.28 eV compared to the 2.97 eV gap for C_{18}. For both molecules, the in-plane conductance through the center of the molecule is greater than the ring conductance. The difference in the sizes of HOMO-LUMO gap for these two molecules is illustrated in Fig. 6. The current-constrained steady state is generated by the mixing of the HOMO and LUMO, so a larger energy gap between these orbitals increases the reorganization energy due to the current constraint. While experimental conductance values for these molecules are not available, the conductance of cyclo[18]carbon connected to graphene leads was recently studied using an NEGF-DFT method, though conductance values were not explicitly reported. Direct comparison to this work is also difficult as a result of the inclusion of leads in the calculations and the differing treatment of the HOMO-LUMO gap in NEGF-DFT [54].

We are also able to investigate the conductance per molecular orbital for the molecules in question, as shown in Fig. 6. For both molecules a small number of molecular orbitals near the HOMO-LUMO gap are the most involved in conductance. Ten percent of the orbitals contain thirty-nine percent of the current in C_{18} and thirty-seven percent of the current in B_9N_9. These orbitals are a mix of π and σ orbitals which are symmetric or nearly symmetric. The core orbitals and the high-energy virtual orbitals are much less involved in conductance than those near the Fermi level, with the core orbitals carrying on average an order of magnitude less current and the high-energy virtual orbitals carrying as much as four orders of magnitude less current. While implementations of many traditional theories like NEGF-DFT require the selection of an energy range for the conductivity, the current-constrained RDM theory predicts the energy (orbital) channels that support the molecular conductivity.

IV. CONCLUSIONS

In the current-constrained 1-RDM theory the current is added as a constraint to compute the voltage, the opposite of traditional theories, which impose a voltage on the molecule to compute the resulting current. As a result of this change in paradigm, we compute an intrinsic conductance for each molecule, a quantity which depends only upon a molecule's energetic response to the imposed current and its electronic structure. As shown in the results, the intrinsic conductance provides a good starting point for the determination of molecular species which may be useful for molecular electronic applications, as molecules without good intrinsic conductance will not be good experimental conductors. In contrast to the quasiparticle description of NEGF-DFT methods, the current-constrained 1-RDM theory directly imposes the necessary boundary conditions for electron trans-
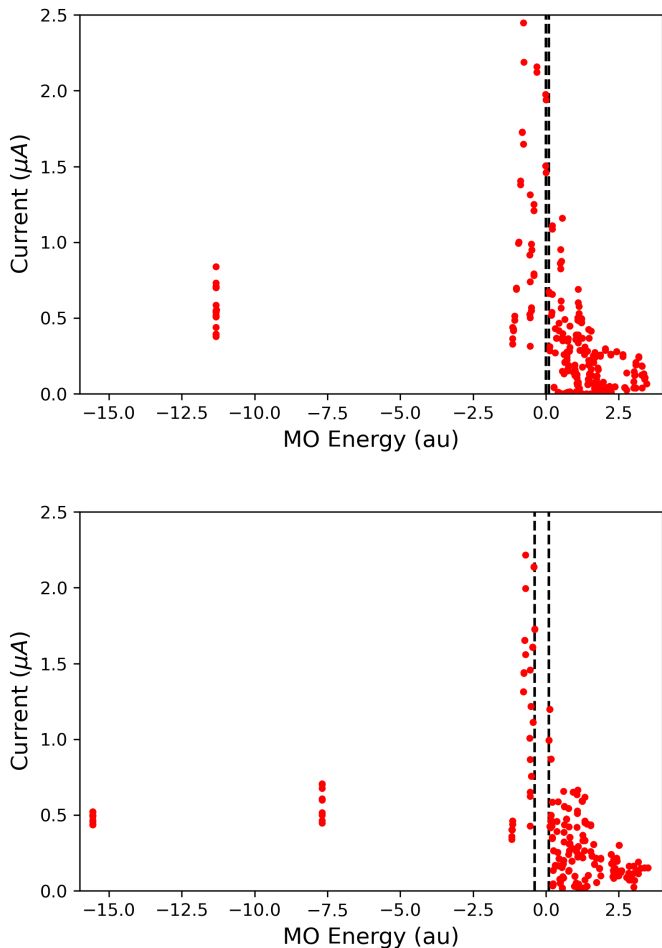

FIG. 6. Current per MO as a function of MO energy for C_{18} (top) and B_9N_9 (bottom). In both cases a total of 100 μA of current is imposed on the system. The dashed lines denote the HOMO and LUMO energies.

port [55]. This paradigm gives more control over the barrier height and allows electronic correlation to be included if necessary.

The current-constrained RDM theory also allows for the study of facets of the conductivity which are not easily accessible using traditional theories, including the ring conductance and the orbital and energy localization of the current. The direct computation of the 1-RDM allows us to construct the equivalent of a molecular-orbital diagram in molecular conductivity where the conductance of each orbital is presented as a function of energy. Just as molecular-orbital diagrams provide an intuitive picture for molecular bonding, these molecular-orbital conduction diagrams provide an intuitive picture for molecular conductivity.

In the this work we investigate the electronic structure of cyclo[18]carbon and its boron nitride analogue using the v2RDM-CASSCF method. We find that the molecular geometry of C_{18} obtained from v2RDM optimization agrees with that found in a recent experiment,

and that the key features of its electronic structure are well-described. We apply the current-constrained theory for molecular conductivity to study the ring and in-plane conductivity of these molecules. We find that they have higher in-plane conductivity than ring conductivity and that C_{18} is more conductive than B_9N_9.

Conflicts of Interest: There are no conflicts of interest to declare.

[1] R. Hoffmann, "Extended Hückel theory—V: Cumulenes, polyenes, polyacetylenes and Cn," Tetrahedron **22**, 521–538 (1966).

[2] P. W. Fowler, N. Mizoguchi, D. E. Bean, and R. W. A. Havenith, "Double aromaticity and ring currents in all-carbon rings," Chem. Eur. J. **15**, 6964–6972 (2009).

[3] G. V. Baryshnikov, R. R. Valiev, A. V. Kuklin, D. Sundholm, and H. Ågren, "Cyclo [18] carbon: Insight into electronic structure, aromaticity, and surface coupling," J. Phys. Chem. Lett. **10**, 6701–6705 (2019).

[4] K. Kaiser, L. M. Scriven, F. Schulz, P. Gawel, L. Gross, and H. L. Anderson, "An sp-hybridized molecular carbon allotrope, cyclo [18] carbon," Science **365**, 1299–1301 (2019).

[5] J. Hutter, H. P. Luethi, and F. Diederich, "Structures and vibrational frequencies of the carbon molecules c_2-c_{18} calculated by density functional theory," J. Am. Chem. Soc. **116**, 750–756 (1994).

[6] M. Saito and Y. Okamoto, "Second-order jahn-teller effect on carbon $4n + 2$ member ring clusters," Phys. Rev. B **60**, 8939 (1999).

[7] C. Neiss, E. Trushin, and A. Görling, "The nature of one-dimensional carbon: Polyynic versus cumulenic," Chem. Phys. Chem **15**, 2497–2502 (2014).

[8] V. Parasuk, J. Almlof, and M. W Feyereisen, "The [18] all-carbon molecule: Cumulene or polyacetylene?" J. Am. Chem. Soc. **113**, 1049–1050 (1991).

[9] F. Diederich, Y. Rubin, C. B. Knobler, R. L. Whetten, K. E. Schriver, K. N. Houk, and Y. I. Li, "All-carbon molecules: evidence for the generation of cyclo[18]carbon from a stable organic precursor," Science **245**, 1088–1090 (1989).

[10] D. A. Plattner and K. N. Houk, "C18 is a polyyne," J. Am. Chem. Soc. **117**, 4405–4406 (1995).

[11] T. Torelli and L. Mitas, "Electron correlation in c_{4n+2} carbon rings: aromatic versus dimerized structures," Phys. Rev. Lett. **85**, 1702 (2000).

[12] S. Arulmozhiraja and T. Ohno, "Ccsd calculations on c_{14}, c_{18}, and c_{22} carbon clusters," J. Chem. Phys. **128**, 114301 (2008).

[13] L. M. Scriven, K. Kaiser, F. Schulz, A. J. Sterling, S. L. Woltering, P. Gawel, K. E. Christensen, H. L. Anderson, and L. Gross, "Synthesis of cyclo [18] carbon via debromination of c18br6," J. Am. Chem. Soc. (2020).

[14] S. Hussain, H. Chen, Z. Zhang, and H. Zheng, "Vibrational spectra and chemical imaging of cyclo[18]carbon by tip enhanced raman spectroscopy," Chem. Commun. **56**, 2336–2339 (2020).

[15] D. L. Strout, "Structure and stability of boron nitrides: the crossover between rings and cages," J. Phys. Chem A **105**, 261–263 (2001).

[16] J. M. L. Martin, J. El-Yazal, and J.-P. François, "Structure and vibrations of $b_n n_n$ (n= 3–10)," Chem. Phys. Lett. **248**, 95–101 (1996).

[17] M. G. Giuffreda, M. S. Deleuze, and J.-P. François, "Structural, rotational, and vibrational properties of mixed ionized boron-nitrogen clusters $b_n n_n^+$ (n= 3- 10)," J. Phys. Chem. A **104**, 5855–5860 (2000).

[18] F. Pichierri, "Boron-nitrogen analogues of cyclo [18] carbon," Chem. Phys. Lett. **738**, 136860 (2020).

[19] D. A Mazziotti, "First-order semidefinite programming for the direct determination of two-electron reduced density matrices with application to many-electron atoms and molecules," J. Chem. Phys. **121**, 10957–10966 (2004).

[20] D. A. Mazziotti, "Realization of quantum chemistry without wave functions through first-order semidefinite programming," Phys. Rev. Lett. **93**, 213001 (2004).

[21] G. Gidofalvi and D. A. Mazziotti, "Active-space two-electron reduced-density-matrix method: Complete active-space calculations without diagonalization of the N-electron Hamiltonian," J. Chem. Phys. **129**, 134108 (2008).

[22] D. A. Mazziotti, "Large-scale semidefinite programming for many-electron quantum mechanics," Phys. Rev. Lett. **106**, 083001 (2011).

[23] D. A. Mazziotti, "Structure of fermionic density matrices: Complete N-representability conditions," Phys. Rev. Lett. **108**, 263002 (2012).

[24] M. Sajjan and D. A. Mazziotti, "Current-constrained density-matrix theory to calculate molecular conductivity with increased accuracy," Commun. Chem. (Nature) **1**, 31 (2018).

[25] A. E. Raeber and D. A. Mazziotti, "Current-constrained one-electron reduced density-matrix theory for non-equilibrium steady-state molecular conductivity," Phys. Chem. Chem. Phys. **21**, 12620–12624 (2019).

[26] A. W. Schlimgen, C. W. Heaps, and D. A. Mazziotti, "Entangled electrons foil synthesis of elusive low-valent vanadium oxo complex," J. Phys. Chem. Lett. **7**, 627–631 (2016).

[27] J. M. Montgomery and D. A. Mazziotti, "Strong electron

correlation in nitrogenase cofactor, femoco," J. Phys. Chem. A **122**, 4988–4996 (2018).

[28] J.-N. Boyn, J. Xie, J. S. Anderson, and D. A. Mazziotti, "Entangled electrons drive a non-superexchange mechanism in a cobalt quinoid dimer complex," J. Phys. Chem. Lett. **11**, 4584–4590 (2020).

[29] A. Aviram and M. A. Ratner, "Molecular rectifiers," Chem. Phys. Lett. **29**, 277–283 (1974).

[30] J. Chen, M. A. Reed, A. M. Rawlett, and J. M. Tour, "Large on-off ratios and negative differential resistance in a molecular electronic device," Science **286**, 1550–1552 (1999).

[31] J. M. Tour, A. M. Rawlett, M. Kozaki, Y. Yao, R. C. Jagessar, S. M. Dirk, D. W. Price, M. A. Reed, C-W. Zhou, J. Chen, W. Wang, and I. Campbell, "Synthesis and preliminary testing of molecular wires and devices," Chem. Eur. J. **7**, 5118–5134 (2001).

[32] A. Batra, P. Darancet, Q. Chen, J. S. Meisner, J. R. Widawsky, J. B. Neaton, C. Nuckolls, and L. Venkataraman, "Tuning rectification in single-molecular diodes," Nano Lett. **13**, 6233–6237 (2013).

[33] D. Xiang, X. Wang, C. Jia, T. Lee, and X. Guo, "Molecular-scale electronics: from concept to function," Chem. Rev. **116**, 4318–4440 (2016).

[34] L.-Y. Hsu, B.-Y. Jin, C.-H. Chen, and S.-M. Peng, "Reaction: new insights into molecular electronics," **3**, 378–379 (2017).

[35] J. Taylor, H. Guo, and J. Wang, "Ab initio modeling of quantum transport properties of molecular electronic devices," Phys. Rev. B **63**, 245407 (2001).

[36] P. S. Damle, A. W. Ghosh, and S. Datta, "Unified description of molecular conduction: From molecules to metallic wires," Phys. Rev. B **64**, 201403 (2001).

[37] M. Di Ventra and Norton D. Lang, "Transport in nanoscale conductors from first principles," Phys. Rev. B **65**, 045402 (2001).

[38] Y. Xue, S. Datta, and M. A. Ratner, "First-principles based matrix green's function approach to molecular electronic devices: general formalism," Chem.Phys. **281**, 151 – 170 (2002).

[39] M. Brandbyge, J-L. Mozos, P. Ordejón, J. Taylor, and K. Stokbro, "Density-functional method for nonequilibrium electron transport," Phys. Rev. B **65**, 165401 (2002).

[40] K. Varga, "Time-dependent density functional study of transport in molecular junctions," Phys. Rev. B **83**, 195130 (2011).

[41] A. E. Rothman and D. A. Mazziotti, "Nonequilibrium,

steady-state electron transport with N-representable density matrices from the anti-hermitian contracted Schrödinger equation," J. Chem. Phys. **132**, 104112 (2010).

[42] E. P. Hoy, D. A. Mazziotti, and T. Seideman, "Development and application of a 2-electron reduced density matrix approach to electron transport via molecular junctions," J. Chem. Phys. **147**, 184110 (2017).

[43] A. J. Coleman, "Structure of fermion density matrices," Rev. Mod. Phys. **35**, 668–686 (1963).

[44] A. J. Coleman and V. I. Yukalov, *Reduced density matrices: Coulson's challenge*, Vol. 72 (Springer Science & Business Media, 2000).

[45] M. Piris, "Global method for electron correlation," Phys. Rev. Lett. **119**, 063002 (2016).

[46] C. L. Benavides-Riveros and C. Schilling, "Natural extension of hartree–fock through extremal 1-fermion information: overview and application to the lithium atom," Z. Phys. Chem. **230**, 703–717 (2016).

[47] C. Schilling, "Relating the pure and ensemble density matrix functional," J. Chem. Phys. **149**, 231102 (2018).

[48] Z. Zhao, B. J. Braams, M. Fukuda, M. L. Overton, and J. K. Percus, "The reduced density matrix method for electronic structure calculations and the role of three-index representability conditions," J. Chem. Phys. **120**, 2095 (2004).

[49] T. H. Dunning Jr., "Gaussian basis sets for use in correlated molecular calculations. i. the atoms boron through neon and hydrogen," The Journal of chemical physics **90**, 1007–1023 (1989).

[50] Philip E Gill, Walter Murray, and Michael A Saunders, "Snopt: An sqp algorithm for large-scale constrained optimization," SIAM review **47**, 99–131 (2005).

[51] Anthony W Schlimgen and David A Mazziotti, "Analytical gradients of variational reduced-density-matrix and wavefunction-based methods from an overlap-reweighted semidefinite program," The Journal of Chemical Physics **149**, 164111 (2018).

[52] Maplesoft, a division of Waterloo Maple Inc., Waterloo, Ontario., "Quantum Chemistry Toolbox from RDM-Chem," (2020).

[53] Maplesoft, a division of Waterloo Maple Inc., Waterloo, Ontario., "Maple," (2020).

[54] L. Zhang, H. Li, Y. P. Feng, and L. Shen, "Diverse transport behaviors in cyclo [18] carbon–based molecular devices," J. Phys. Chem. Lett. (2020).

[55] P Delaney and James C Greer, "Correlated electron transport in molecular electronics," Physical review letters **93**, 036805 (2004).